Published in final edited form as:

J Immunol. 2018 August 01; 201(3): 930–939. doi:10.4049/jimmunol.1800054.

VprBP/DCAF1 Regulates RAG1 Expression Independently of Dicer by Mediating RAG1 Degradation

N. Max Schabla[*], **Greg A. Perry**[*], **Victoria L. Palmer**[*], and **Patrick C. Swanson**[*]

[*]Department of Medical Microbiology and Immunology, Creighton University, 2500 California Plaza, Omaha, NE, USA 68178

Abstract

The assembly of immunoglobulin genes in developing B lymphocytes by V(D)J recombination is initiated by the RAG1-RAG2 endonuclease complex. We previously identified an interaction between RAG1 and VprBP/DCAF1, a substrate receptor for the Cullin 4-RING E3 ubiquitin ligase (CRL4). We report here that in mice, B cell-intrinsic loss of VprBP/DCAF1 increases RAG1 protein levels and disrupts expression of the endoribonuclease Dicer, which is essential for miRNA maturation. *Rag1/2* transcription is known to be de-repressed by loss of miRNA-mediated suppression of PTEN, raising the possibility that the elevated level of RAG1 observed in VprBP/DCAF1-deficient B cells is caused indirectly by the loss of Dicer. However, we show that VprBP/DCAF1 restrains RAG1 expression post-transcriptionally and independently of Dicer. Specifically, loss of VprBP/DCAF1 stabilizes RAG1 protein, which we show is normally degraded via a mechanism requiring both 20S proteasome and Cullin-RING E3 ubiquitin ligase (CRL) activity. Furthermore, we show that RAG1 stabilization through small molecule inhibition of CRL activation promotes V(D)J recombination in a murine pre-B cell line. Thus, in addition to identifying a role for VprBP/DCAF1 in maintaining Dicer levels in B cells, our findings reveal the basis for RAG1 turnover, and provide evidence that the $CRL4^{VprBP/DCAF1}$ complex functions to maintain physiological levels of V(D)J recombination.

Keywords

RAG1 half-life; RAG1 expression; V(D)J recombination; B cell development; CRL4 E3 ubiquitin ligase

Introduction

The generation of a diverse lymphocyte antigen receptor repertoire is fundamental to adaptive immunity. Developing B cells assemble functional immunoglobulin (Ig) genes from arrays of variable (V), diverse (D), and joining (J) segments via an orchestrated process of DNA cleavage and joining called V(D)J recombination (1). The process is initiated by the recombination activating gene proteins 1 and 2 (RAG1 and RAG2), which together comprise

Correspondence: Patrick C. Swanson, Ph.D., Department of Medical Microbiology and Immunology, Creighton University, 2500 California Plaza, Omaha, NE, USA 68178, Phone: (402)-280-2716, FAX: (402)-280-1875, pswanson@creighton.edu.

Disclosures

The authors declare no financial conflicts of interest.

the site-specific endonuclease that introduces DNA double strand breaks at the recombination signal sequences (RSSs) flanking Ig gene segments (2, 3). The amino-terminal region (NTR) of RAG1, spanning aa1-383, is dispensable for RAG catalytic activity *in vitro* (4, 5). However, deletion of the NTR impairs the efficiency and fidelity of V(D)J recombination and reduces peripheral B and T cell numbers *in vivo* (6–9).

A mechanistic understanding for how the RAG1 NTR contributes to maintaining normal levels of V(D)J recombination and lymphocyte development remains incomplete. The discovery that the RAG1 NTR contains a functional RING domain (10), which is characteristic of E3 ubiquitin ligases that catalyze the transfer of ubiquitin to substrate proteins (11), raised the possibility that RAG1 mediates ubiquitylation of itself and/or other target proteins to facilitate V(D)J recombination. Indeed, evidence supporting both possibilities has been published: RAG1 is reported to undergo auto-ubiquitylation (12), which may stimulate its V(D)J recombination activity (12–14), and has also been implicated in mediating ubiquitylation of other proteins, including the nuclear transport protein karyopherin-α (15) and histone H3 (16, 17). However, the relationship between substrate ubiquitylation and V(D)J recombination *in vivo* remains unclear.

A second, non-mutually exclusive functional role for the NTR is as a protein-protein interaction domain used to recruit accessory factors that enhance or regulate V(D)J recombination (18–21). The functional significance of these interactions is not fully understood. We previously identified an association between the RAG1 NTR and Viral protein r Binding Protein/DNA Damage Binding Protein 1 (DDB1)-Cullin 4 (Cul4) Associated Factor 1 (VprBP/DCAF1; VprBP henceforth), a substrate receptor for the Cul4-RING (Really Interesting New Gene) E3 ubiquitin ligase (CRL4) (21). We further showed that when mb1-Cre transgene expression (22) is used to conditionally inactivate *Vprbp* in murine B cells (henceforth called VprBP$^{del/del}$ mice), B cell development is blocked at the pro- to pre-B cell transition, and distal V_H-DJ_H and V_κ-J_κ gene rearrangement is impaired (21).

More recently, we reported that the developmental block in VprBP$^{del/del}$ mice could be partially bypassed by enforced expression of Bcl2 (henceforth called VprBP$^{del/del}$ Bcl2$^+$ mice), which also restored distal V gene rearrangement at both the *Igh* and *Igk* loci (23). Interestingly, most B cells reaching the periphery in VprBP$^{del/del}$ Bcl2$^+$ mice are Igλ$^+$, reflecting a ~10-fold loss in the absolute number of splenic Igκ$^+$ B cells. This outcome is correlated with increased levels of secondary V(D)J rearrangements in the *Igk* locus, including κ-deletion and skewing of Vκ rearrangements to Jκ5, as well as elevated rearrangement of the *Igl* locus (23). These secondary V(D)J rearrangements are often associated with receptor editing, which can be initiated in response to ligation of the BCR by self-antigen at the immature B cell stage (24), raising the possibility that loss of VprBP in VprBP$^{del/del}$ Bcl2$^+$ mice leads to excessive V(D)J recombination and receptor editing.

The skewing of the B cell repertoire toward Igλ$^+$ B cells observed in VprBP$^{del/del}$Bcl2$^+$ mice is also reminiscent of what is observed in Bcl2-transgenic mice with a B-lineage deficiency in the the DiGeorge critical region 8 (DGCR8) protein (25), a component of the microprocessor complex essential for producing mature microRNAs (miRNAs) (26). This

outcome was traced to de-repression of *Rag* expression and excessive receptor editing caused indirectly by the loss of miRNA-mediated silencing of phosphatase and tensin homologue (PTEN), a lipid phosphatase that antagonizes phosphoinositide-3-kinase (PI3K) signaling (25).

Consistent with the possibility that excessive V(D)J recombination is a causal factor that explains the phenotype observed in VprBP$^{del/del}$Bcl2^{+} mice, we show here that RAG1 protein levels are elevated in bone marrow (BM) B cells cultured from VprBP$^{del/del}$Bcl2^{+} mice. In the same cells, we show a severe reduction in the protein level of the endoribonuclease Dicer, another factor which is essential for miRNA biogenesis (26). This raised the possibility that the skewed Igκ:Igλ ratio and excessive receptor editing observed in VprBP$^{del/del}$Bcl2^{+} mice is a secondary effect caused by Dicer loss in developing B cells. However, the increase in RAG1 protein under these conditions was not correlated with elevated *Rag1* transcript levels. Furthermore, while we observed increased levels of *Rag1* transcript and RAG1 protein in splenic B cells from Bcl2-transgenic mice with a B lineage-specific deficiency in Dicer (henceforth called Dicer$^{del/del}$Bcl2^{+} mice), which is consistent with results reported by Coffre *et al.* (25), splenic B cells from VprBP$^{del/del}$Bcl2^{+} mice showed no increase in *Rag1* transcript yet RAG1 protein remained elevated. Moreover, RAG1 protein levels were not elevated in cultured BM B cells from Dicer$^{del/del}$Bcl2^{+} mice. Instead, we found that loss of VprBP expression extended the half-life of the RAG1 protein, and that turnover of RAG1 was proteasome-dependent and required Nedd8-dependent activation of Cullin-RING E3 ubiquitin ligases (CRLs). These results suggest a model in which VprBP regulates RAG1 turnover by directing its proteasomal degradation via the activated CRL4 complex.

We conclude that while both VprBP and Dicer negatively regulate RAG1 expression in order to restrain excessive RAG activity, they do so through distinct mechanisms: VprBP controls RAG1 expression post-translationally via proteasome-dependent degradation, whereas Dicer suppresses *Rag* transcription. We speculate that these mechanisms operate at different stages of B cell ontogeny, with VprBP being crucial for suppressing RAG1 in pre-B and immature B cells, and Dicer functioning to control RAG expression in peripheral B cells. Our findings reveal previously unidentified roles for VprBP in maintaining Dicer protein levels during B cell development, and in regulating V(D)J recombination by mediating RAG1 turnover.

Materials and Methods

Mice

The generation of VprBP$^{fl/fl}$Bcl2^{+} and VprBP$^{del/del}$Bcl2^{+} mice has been described (23, 27). Mice bearing conditional *Dicer* alleles (28) (B6.Cg-*Dicer1*^{tm1Bdh}/J; Dicer$^{fl/fl}$ mice henceforth) were purchased from the Jackson Laboratory. In order to generate Dicer$^{del/del}$Bcl2^{+} mice and littermate controls, Dicer$^{fl/fl}$ mice were initially crossed with VprBP$^{fl/fl}$Bcl2^{+} and VprBP$^{del/del}$ mice, to breed on the Bcl2 or mb1-Cre transgene onto the Dicer^{fl} background, and then successively back-crossed to remove the conditional *Vprbp* alleles. The resulting Dicer$^{fl/fl}$Bcl2^{+} and Dicer$^{del/del}$ mice were crossed to generate mice for analysis. All mice were housed in individually ventilated microisolator cages in an American Association for the Accreditation of Laboratory Animal Care-certified facility at

Creighton University. For all experiments, control and knockout animals were either co-housed littermates or were derived from parallel breedings. All experimental procedures were reviewed and approved by the Creighton University Institutional Animal Care and Use Committee.

Bone marrow culture

Mice were sacrificed by cervical dislocation at 6–8wk of age and bone marrow cells were flushed from the femora and tibiae. Cells were prepared as described (29). Briefly, adherent cells were removed by incubating collected bone marrow cells at 37 °C for 15min. Non-adherent cells were collected by centrifugation, subjected to red blood cell lysis in ACK Lysing Buffer (Thermo Fisher), washed, and seeded at a density of 7.5×10^5/mL in 1X Iscove's Modified Dulbecco's Medium (IMDM) supplemented with 10% fetal bovine serum (Life Technologies), 1X penicillin/streptomycin (Corning), 2mM L-glutamine (Sigma-Aldrich), 5.5×10^{-5} M β-mercaptoethanol (Sigma-Aldrich), and 10 ng/μl of recombinant murine IL-7 (R&D systems). Cells were cultured at 37 °C with 5% CO_2 for two consecutive periods of 4d, with cells being re-seeded at their initial density after the first culture period. For experiments including IL-7 withdrawal, cells were washed twice in 10 mL of culture medium and re-seeded at 7.5×10^5/ml in fresh medium containing 20 ng/μl of recombinant murine B cell activating factor (BAFF, R&D systems) and cultured 2d prior to analysis.

Flow Cytometry and Cell Sorting

Single-cell suspensions prepared from bone marrow or spleen of 6–8wk old mice, or cultured bone marrow cells were analyzed by multicolor immunophenotyping. To detect surface antigens, cells were Fc-blocked using anti-CD16/32 (2.4G2, Becton Dickenson) and stained with the following fluorochrome-conjugated antibodies: eBioscience anti-TCRβ-PE (H57-597), anti-CD19-AlexaFluor700 (eBio1D3), anti-IgM-PE-Cy5 (Il/41), anti-CD93-PE-Cy7 (AA4.1), Becton-Dickinson anti-B220-PE-CF594 (RA3-6B2), anti-CD43-APC (S7), anti-Igκ-PerCP-Cy5.5 (187.1), anti-CD21/CD35-APC (7G6), biotinylated anti-CD23 (B3B4) detected with BV510-Streptavidin, anti-Igλ-FITC (R26-46) and BioLegend anti-IgD-APC-Cy7 (11-26c.2a). For detecting intracellular PTEN, cells were fixed and permeabilized after surface staining using the CytoFix/CytoPerm kit (Becton-Dickinson) according to manufacturer instructions. Permeabilized cells were stained with anti-PTEN-AlexaFluor488 (IC847G, Novus Biologicals) or isotype control antibody (MOPC-21, eBioscience). All samples were stained with violet-fluorescent LIVE/DEAD dye (Life Technologies) for discrimination of non-viable cells. All phenotypic analyses were performed using a ZE5 Analyzer (Bio-Rad). For these analyses, B cells were defined as live, $B220^+CD19^+TCR\beta^-$ cells within a lymphocyte gate. For sorting of splenic B cells, splenocytes were stained with Becton-Dickenson antibodies anti-B220-PE (RA3-6B2), anti-CD19-APC-Cy7 (1D3) and anti-CD25-APC-R700 (PC61), and $B220^+CD19^+CD25^-$ B cells were sorted using a FACSAria (Becton-Dickinson). Sorting of bone marrow was performed after staining cells with Becton Dickenson antibodies anti-B220-PE (RA3-6B2), anti-IgM-PE-Cy5 (Il/41), and anti-CD43-biotin (S7) detected using BUV737-conjugated streptavidin. Pre-B cells were sorted as $B220^+CD43^-IgM^-$. All data generated in phenotyping and sorting experiments were analyzed using the FlowJo software package (Treestar). For cell cycle analysis, $VprBP^{fl/fl}Bcl2^+$ and $VprBP^{del/del}Bcl2^+$ BM cultures were subjected to B cell

enrichment by magnetic sorting (Miltenyi Biotec) to remove residual non-B cells. Purified B cells were resuspended in Vindelov's reagent (100mM Tris, 0.9% NaCl, 0.01mg/mL RNase A, 0.075mg/mL propidium iodide, 0.1% NP-40) and analyzed on the ZE5. Cell cycle modeling was performed using the ModFit program (Verity Software House).

Western blot analysis

Cultured or sorted cells ($2–4\times10^6$) were incubated for 10min on ice in RIPA lysis buffer (50mM Tris, 150mM NaCl, 1% NP-40, 0.5% sodium deoxycholate, 0.1% SDS, 1mM EDTA) supplemented with 1mM sodium orthovanadate and 2% v/v protease inhibitor cocktail (Sigma-Aldrich P8340). Proteins were resolved by SDS-PAGE prior to transfer onto PVDF membrane and detection. The following primary antibodies were used: Anti-Dicer (Bethyl Laboratories, A301-936A), anti-VprBP (Proteintech group, 11612-I-AP), anti-RAG1 (rabbit mAb developed by the Schatz group, see (18)), anti-RAG2 (EMD Millipore, MABE1104), and anti-β-actin (Sigma-Aldrich, A5316). HRP-conjugated goat-anti-rabbit or anti-mouse secondary antibodies (Cell Signaling Technology) were used to detect primary antibody, and blots were developed using Pierce ECL2 substrate (Thermo-Fisher) and imaged using a Typhoon 9410 Variable Mode Imager (GE Healthcare). All western blot signal quantification was performed using the ImageJ image processing tool (https://imagej.NIH.gov).

RT-qPCR analysis

Total RNA was isolated from cultured BM cells or sorted splenic B cells using the GenElute Mammalian Total RNA Miniprep kit (Sigma-Aldrich). cDNA was prepared using Taqman Reverse Transcription Reagents (Life Technologies). qPCR reactions were set up using 2X SYBR Green Mastermix (Thermo-Fisher) and carried out on a CFX96 Real-Time system (Bio-Rad) with the following thermal cycling conditions: 95 °C for 1min, followed by 35 cycles of 95 °C for 30sec, 55 °C for 15sec and 72 °C for 15sec. Data were analyzed using software accompanying the instrument. The following primer pairs were used for RT-qPCR assays (30, 31) (OriGene Technologies, MP203654):

Primer Name	Sequence
Rag1 – F	5′-ATGGCTGCCTCCTTGCCGTCTACC-3′
Rag1 – R	5′-CTGAGGAATCCTTCTCCTTCTGTG-3′
Rag2 – F	5′-TTAATTCCTGGCTTGGCCG-3′
Rag2 – R	5′-TTCCTGCTTGTGGATGTGAAAT-3′
Dicer – F	5′-AGCAGTGCTGAGAAGAGGAAGG-3′
Dicer – R	5′-CCGCTTTTCTCCACAGTGATGC-3′
Hprt – F	5′-CTGGTGAAAAGGACCTCTCG-3′
Hprt – R	5′-TGAAGTACTCATTATAGTCAAGGGCA-3′

PCR-southern blot analysis of V(D)J rearrangements

Genomic DNA was prepared from sorted splenic B cells and specific V(D)J rearrangements were amplified from 10000, 2500, or 625 cell equivalents in PCRs with primer sets and

thermal cycling conditions as previously described (23). For PCR amplification of Vκ-RS rearrangements, the RS primer (23) was paired with a degenerate Vκ primer (5′-GGCTGCAGSTTCAGTGGCAGTGGRTCWGGRAC-3′, ref. (32)), and thermal cycling conditions identical to those for IRS-RS were used (23). PCR products were transferred to nitrocellulose membranes, hybridized with ^{32}P labeled oligonucleotide probes, and detected by autoradiography.

RAG1 protein half-life experiments

BM cells from VprBP$^{fl/fl}$Bcl2^{+} or VprBP$^{del/del}$Bcl2^{+} mice were expanded 8d in the presence of IL-7, followed by 48h of culture in medium lacking IL-7 and supplemented with BAFF as described above. At 24h following IL-7 withdrawal, MLN4924 (Selleckchem, 3μM), Bortezomib (Selleckchem, 5μM), or DMSO (vehicle control) was added and cells were cultured for an additional 24h. Cycloheximide (CHX, 20 μg/ml, Sigma-Aldrich) was added for the final 2h of the culture period, and cells were harvested at 30 min intervals. For experiments using the A70 cell line (33), cells were seeded at a density of 1×10^{6}/mL in RPMI medium supplemented with 10% fetal bovine serum (Life Technologies), 1X penicillin/streptomycin (Corning), 2mM L-glutamine (Sigma-Aldrich), 5.5×10^{-5} M β-mercaptoethanol (Sigma-Aldrich). Cells were cultured with STI-571 (Tocris Bioscience, 5μM) for 24h, and then cultured for an additional 24h in the presence of MLN4924 (3μM) or DMSO (vehicle control). For the final 2h, CHX (20μg/mL) was added, and cells were harvested at 30 min intervals.

Statistics

Data are presented as mean values +/− SEM. All data were analyzed by ANOVA with Bonferroni Correction using the GraphPad Prism platform. P-values of ≤ 0.05 were considered significant.

Results

VprBP controls expression of RAG1 and Dicer in developing B cells

Our previous observation that κ-deletion was elevated in sorted Igκ^{+} B cells from VprBP$^{del/del}$Bcl2^{+} mice (23) raised the possibility that the skewed Igκ^{+}:Igλ^{+} ratio on this genetic background is caused by excessive RAG activity. To explore this possibility, we used a stromal cell-independent BM culture system in which pro- and pre-B cells are expanded in the presence of recombinant IL-7 for 8d (8d+IL-7), and then cultured for an additional 2d after substituting IL-7 for recombinant BAFF (2d+BAFF) (29). IL-7 withdrawal has been shown to stimulate transit from the large- to small-pre-B cell stage and upregulate *Rag* expression, while BAFF enhances cell survival in the absence of IL-7 (29, 34, 35). Compared to 0d cultures, the 8d+IL-7 BM cultures from VprBP$^{fl/fl}$Bcl2^{+} and VprBP$^{del/del}$Bcl2^{+} mice showed substantial enrichment of B220^{+}CD19^{+} cells, which persisted in the 2d+BAFF cultures (Fig. 1A). Cells from VprBP$^{fl/fl}$Bcl2^{+} and VprBP$^{del/del}$Bcl2^{+} mice showed very similar cell cycle profiles when cultured under both conditions (Fig. 1B); IL-7 withdrawal led to an increase in the percentage of cells in the G1 phase of the cell cycle for both genotypes. Western blotting of cell lysates prepared from both the 8d+IL-7 and the 2d+BAFF BM cultures revealed the presence of VprBP in samples

from VprBP$^{fl/fl}$Bcl2^{+} mice, but not VprBP$^{del/del}$Bcl2^{+} mice (Fig. 1C). Interestingly, RAG1 protein was elevated ~6-fold in 8d+IL-7 BM cultures from VprBP$^{del/del}$Bcl2^{+} mice relative to VprBP$^{fl/fl}$Bcl2^{+} mice (Fig. 1C–D), but levels of *Rag1* transcript were not significantly different in these samples (Fig. 1E). Withdrawal of IL-7 stimulated a ~10-fold increase in *Rag1* transcript in VprBP$^{fl/fl}$Bcl2^{+} cells, which was accompanied by a ~3-fold increase in RAG1 protein levels (Fig 1C–E). By contrast, VprBP$^{del/del}$Bcl2^{+} cells failed to robustly induce *Rag1* transcription, showing significantly lower expression than VprBP$^{fl/fl}$Bcl2^{+} cells after IL-7 withdrawal (Fig. 1E). Notably, despite poor *Rag1* transcriptional induction, RAG1 protein levels in these samples were ~3-fold higher than in comparable samples from VprBP$^{fl/fl}$Bcl2^{+} mice (Fig. 1C–D). In these samples, RAG2 protein levels were similar between VprBP-proficient and VprBP-deficient cells (Fig. 1C), whereas the levels of *Rag2* transcript followed a similar pattern as observed for *Rag1* (Fig. 1E).

Recent work by the Koralov group suggests that *Rag* expression is constrained at the transcriptional level indirectly through miRNA-mediated suppression of PTEN (25). They further reported that loss of miRNAs in B cells skews the ratio of Igκ^{+}:Igλ^{+} cells toward Igλ^{+} B cells, a feature that resembles what we previously observed in VprBP$^{del/del}$Bcl2^{+} mice (23). Two reports indicating a role for VprBP in directing ubiquitin-dependent degradation of Dicer in response to certain stimuli (36, 37) suggested a potential mechanistic link between *Rag* expression and VprBP through its regulation of Dicer-mediated miRNA biogenesis. This prompted us to investigate whether Dicer expression was altered in VprBP-deficient B cell progenitors. Strikingly, we found that Dicer is undetectable by western blot in VprBP$^{del/del}$Bcl2^{+} BM cells cultured under both the 8d+IL-7 and 2d+BAFF conditions (Fig. 1C). The effect of VprBP deficiency on Dicer protein levels is independent of transcription, as there is no significant difference in *Dicer* mRNA levels between VprBP$^{fl/fl}$Bcl2^{+} and VprBP$^{del/del}$Bcl2^{+} BM cultured under either condition (Fig. 1F). Taken together, these data suggest that VprBP suppresses RAG1 expression post-transcriptionally, and is necessary for efficient transcriptional upregulation of *Rag1* upon attenuation of IL-7 receptor signaling. Furthermore, VprBP is necessary for maintaining cellular Dicer levels in a manner that is independent of *Dicer* transcription.

VprBP and Dicer restrain excessive RAG activity through distinct mechanisms

The previous data suggest that the increase in RAG1 protein observed in VprBP$^{del/del}$Bcl2^{+} B cells is not a secondary effect of Dicer loss that results in *Rag* transcriptional upregulation. To test this more directly, we generated Dicer$^{fl/fl}$Bcl2^{+} and Dicer$^{del/del}$Bcl2^{+} mice as reported previously (25, 38), and compared them to VprBP$^{fl/fl}$Bcl2^{+} and VprBP$^{del/del}$Bcl2^{+} mice (Fig. 2). B220^{+}CD19^{+} B cells account for ~60% and ~40% of live TCRβ^{-} splenocytes in VprBP$^{del/del}$Bcl2^{+} and Dicer$^{del/del}$Bcl2^{+} mice, respectively (Fig. 2A, top panels). The percentage of B cells expressing surface Ig was higher in VprBP$^{del/del}$Bcl2^{+} mice expressed compared to Dicer$^{del/del}$Bcl2^{+} mice (Fig. 2A, middle panels). Nevertheless, the absolute number of splenic B cells, and the absolute numbers of Igκ^{+} and Igλ^{+} B cells, were not significantly different between these two genetic backgrounds (Fig. 2B, left and right panels, respectively). Consistent with the phenotype of Bcl2-transgenic DGCR8-deficient B cells reported previously (25), splenic B cells from Dicer$^{del/del}$Bcl2^{+} mice express low levels of

surface IgM, but this feature is not recapitulated in splenic B cells from VprBP$^{del/del}$Bcl2^{+} mice (Fig. 2C).

In VprBP$^{del/del}$Bcl2^{+} and Dicer$^{del/del}$Bcl2^{+} mice, the ratio of Igκ^{+}:Igλ^{+} cells was observed to be ~1:3 and ~1:1, respectively, whereas it was ~3:1 in both VprBP$^{fl/fl}$Bcl2^{+} and Dicer$^{fl/fl}$Bcl2^{+} mice (Fig. 2A bottom panels and Fig. 2D). As might be expected, levels of intron recombining sequence (IRS)-to-recombining sequence (RS) and Vκ-RS rearrangements leading to κ-deletion (39) were correspondingly increased in sorted B220^{+}CD19^{+}CD25^{-} splenic B cells from both VprBP$^{del/del}$Bcl2^{+} and Dicer$^{del/del}$Bcl2^{+} mice compared to their counterparts lacking mb1-Cre, but were slightly higher in the sorted B cells from VprBP$^{del/del}$Bcl2^{+} mice than those from Dicer$^{del/del}$Bcl2^{+} mice (Fig. 2E). Excessive light chain gene rearrangement in these mice was also evidenced by skewing of Jκ gene segment usage to Jκ5, as well as increased Vλ1-Jλ1 rearrangement (Fig. 2E).

The Koralov group attributed the excessive Ig light chain gene editing phenotype of DGCR8-deficient B cells to increased expression of PTEN, which suppresses PI3K signaling and thereby allows elevated transcription and activity of *Rag*s in the periphery (25). While we observed increased levels of intracellular PTEN in splenic B cells from both VprBP$^{del/del}$Bcl2^{+} mice and Dicer$^{del/del}$Bcl2^{+} mice using flow cytometry (Fig. 2F–G), *Rag1* and *Rag2* transcript levels were only found to be elevated in sorted B cells from Dicer$^{del/del}$Bcl2^{+} mice, and not VprBP$^{del/del}$Bcl2^{+} mice, consistent with the block in *Rag* transcription observed in cultured BM cells from the latter mice (Fig. 2H). Despite low levels of *Rag1* transcript in VprBP$^{del/del}$Bcl2^{+} splenic B cells, RAG1 protein was clearly detected by western blotting in these cells, whereas it was not evident in VprBP$^{fl/fl}$Bcl2^{+} cells (Fig. 2I). Consistent with increased *Rag1* transcript in Dicer$^{del/del}$Bcl2^{+} splenic B cells, RAG1 was also detectable in these cells, albeit at a lower level than in VprBP$^{del/del}$Bcl2^{+} cells (Fig. 2I). Taken together, these data suggest that while both VprBP and Dicer function to constrain V(D)J recombination activity by controlling RAG protein levels, they do so via distinct mechanisms.

Loss of Dicer alone is insufficient to elevate RAG1 expression in cultured BM cells

Given the upregulation of *Rag1* transcript observed in splenic B cells from Dicer$^{del/del}$Bcl2^{+} mice, but not VprBP$^{del/del}$Bcl2^{+} mice, we next wished to determine whether this phenomenon would also be observed in the BM cell culture system. In the 8d+IL-7 cultures, B220^{+}CD19^{+} cells from VprBP$^{del/del}$Bcl2^{+} and Dicer$^{del/del}$Bcl2^{+} mice were enriched to a similar degree (Fig. 3A). Importantly, while the level of RAG1 protein was elevated in cultured VprBP$^{del/del}$Bcl2^{+} BM cells as compared to their VprBP$^{fl/fl}$Bcl2^{+} counterparts, it was diminished in Dicer$^{del/del}$Bcl2^{+} cells (Fig. 3B), suggesting that elevation of RAG1 protein is not secondary to the loss of Dicer on the VprBP$^{del/del}$Bcl2^{+} background. Furthermore, we found that levels of *Rag1* and *Rag2* transcript were slightly diminished in both the VprBP- and Dicer-deficient BM cultures (Fig. 3C). Intracellular PTEN levels were not elevated in either knockout strain, suggesting that miRNAs are not critical for suppressing *Rag* expression at early B cell developmental stages (Fig. 3D–E). Consistent with these observations, marks of receptor editing, including κ-deletion, Igλ rearrangement, and skewing of Vκ-Jκ joins to Jκ5, were elevated in sorted VprBP$^{del/del}$Bcl2^{+} bone marrow

pre-B cells as compared to VprBP$^{fl/fl}$Bcl2^{+} pre-B cells, whereas levels of these rearrangements between Dicer-proficient and –deficient pre-B cells were quite similar (Fig. 3F). We also noted a marked overall decrease in *Igk* rearrangement in Dicer$^{del/del}$Bcl2^{+} pre-B cells as compared to Dicer$^{fl/fl}$Bcl2^{+} counterparts (Fig. 3F), which may be partly attributed to lower RAG1 protein levels observed in Dicer$^{del/del}$Bcl2^{+} BM cultures (Fig. 3B) (see Discussion section). Taken together, these data support a model in which, during early B cell development, VprBP functions to post-transcriptionally regulate RAG1 protein levels, independently of its role in maintaining cellular Dicer levels, whereas in the periphery, Dicer is necessary for proper suppression of *Rag* transcription, but loss of VprBP overrides the effects of an absence of Dicer.

VprBP Is required for normal turnover of RAG1 protein

We next sought to determine the mechanism by which VprBP mediates RAG1 post-transcriptional suppression. A well-established feature of cellular RAG1 is its short half-life of ~10–30 min (40–42). We speculated that loss of VprBP might extend RAG1 half-life, leading to its accumulation. To test this possibility, 2d+BAFF BM cultures from VprBP$^{fl/fl}$Bcl2^{+} and VprBP$^{del/del}$Bcl2^{+} mice were treated with cycloheximide (CHX) for the final 2 hours of the culture period in order to block all protein translation. Lysates prepared from cells harvested at 30 min intervals during CHX treatment were probed for RAG1 protein by immunoblotting. Under these conditions, we observed that RAG1 was degraded with an estimated half-life of ~30 min in VprBP$^{fl/fl}$Bcl2^{+} cells. (Fig. 4A). In striking contrast, RAG1 protein levels in VprBP$^{del/del}$Bcl2^{+} cells remained consistently elevated through the entire 2h CHX treatment period, indicating that VprBP is required for normal turnover of the RAG1 protein (Fig. 4A).

This observation, along with VprBP's established role as a substrate receptor for the CRL4 E3 ubiquitin ligase (reviewed in (43)), raised the possibility that VprBP directs the degradation of RAG1 via the CRL4^{VprBP} complex. To test this possibility, we repeated the experiment with VprBP$^{fl/fl}$Bcl2^{+} cells as shown in Fig. 4A, except that cells were treated during the last 24h of the IL-7 withdrawal period with MLN4924, an inhibitor of the Nedd8-activating E1 enzyme (NAE) (44). The rationale for using this inhibitor is that NAE is required for activating CRL complexes by initiating conjugation of the ubiquitin-like protein Nedd8 to the cullin scaffold (45–47). We found that MLN4924 treatment of VprBP$^{fl/fl}$Bcl2^{+} cells treated under these conditions showed no apparent RAG1 degradation during the period of concomitant CHX treatment, essentially mirroring the effect of loss of VprBP (Fig. 4B). As a control, VprBP$^{fl/fl}$Bcl2^{+} cells treated with vehicle only (DMSO) showed similar turnover kinetics as observed with VprBP$^{fl/fl}$Bcl2^{+} cells in Fig. 4A. Furthermore, RAG2 levels remained largely unchanged during the CHX treatment period, and were not affected by concomitant exposure to MLN4924 (Fig. 4B). In keeping with CRL4^{VprBP}-dependent turnover of RAG1, we found that treatment of VprBP$^{fl/fl}$Bcl2^{+} cells with the proteasome inhibitor Bortezomib (48) extended the half-life of RAG1 to ~130 min compared to ~30 min in the vehicle-treated control (Fig. 4C).

To further extend mechanistic studies of RAG1 turnover, we investigated the effects of MLN4924 treatment in an Abelson murine leukemia virus (AMuLV)-transformed pre-B cell

line called A70 (33). Treatment of AMuLV-transformed pre-B cells with STI-571, a small molecule inhibitor of the vAbl kinase, induces G1 cell cycle arrest and stimulates *Rag* transcription (49). Recapitulating the effects of MLN4924 treatment observed with primary B cells from $VprBP^{fl/fl}Bcl2^{+}$ mice, we found that NAE inhibition in STI-571-treated A70 cells stabilizes RAG1 in the presence of CHX, whereas RAG1 is turned over normally in A70 cells treated with STI-571 and DMSO as the vehicle control (Fig. 4D). Furthermore, the expression and half-life of RAG2 remained unaffected by MLN4924 treatment in STI-571-treated A70 cells (Fig. 4D).

The A70 cells used in these experiments harbor a chromosomally integrated V(D)J recombination reporter substrate consisting of an antisense cDNA encoding GFP flanked by a pair of RSSs, called pMX-INV (33). Upregulation of RAGs upon STI-571 treatment enables inversion and expression of the antisense GFP cDNA (Fig. 4E). Treatment of A70 cells simultaneously with STI-571 and MLN4924 resulted in a ~25% increase in expression of the GFP reporter substrate compared to cells treated with STI-571 and DMSO vehicle control, indicating that the increased half-life of RAG1 promotes increased V(D)J recombination (Fig. 4F). Taken together, these data suggest that VprBP mediates RAG1 turnover through a mechanism that is proteasome-dependent and requires CRL E3 ubiquitin ligase activity.

Discussion

While long recognized, the mechanistic basis for the short half-life of cellular RAG1 has remained obscure. Our findings have provided significant new insight that helps explain this phenomenon, establishing that VprBP, which we previously identified as associating with full-length RAG1 (21), mediates RAG1 degradation through a mechanism that is proteasome-dependent and requires NAE activity. Since NAE-dependent neddylation of cullins is required for their activation, the simplest conclusion is that VprBP promotes RAG1 degradation via the $CRL4^{VprBP}$ complex. What remains to be clarified is the precise mechanism by which RAG1 is directed to the proteasome for degradation.

The short half-life of RAG1 may be a strategy by which developing lymphocytes restrain RAG activity in order to limit off-target cleavage to protect genomic stability. Our observation that loss of VprBP is associated with an increase in Ig light chain gene recombination events and loss of $Ig\kappa^{+}$ B cells also suggests that this mechanism contributes to the proper developmental timing of *Igk* and *Igl* rearrangement. This is an attractive model for two reasons. First, evidence suggests RAG2 is expressed in molar excess to RAG1 (~15-fold); therefore, one would expect the latter to be rate-limiting for V(D)J recombination (50). Indeed, our finding that concomitant treatment of A70 cells with STI-571 and MLN4924 increases RAG1 levels, but not RAG2 levels, and promotes greater V(D)J rearrangement of the GFP reporter substrate in these cells is consistent with this possibility. The finding that *Rag1* heterozygosity reduces receptor editing in a mouse model of enforced autoreactivity (51) also provides additional experimental support for this possibility.

Second, the short half-life of RAG1 may provide a means to restrain V(D)J recombination during a phase of the cell cycle when RAG2 levels are fixed. Specifically, RAG2 is known to

undergo phosphorylation-dependent ubiquitylation and degradation at the G1-to-S phase transition, but is stabilized during G1, the phase of the cell cycle to which V(D)J recombination is restricted (52–54). With CRLs being implicated in the turnover of RAG1, physiological mechanisms may exist to suppress CRL activity during the G1 phase to enable transient upregulation of RAG1 levels. Furthermore, with VprBP also being implicated in controlling *Rag* transcriptional upregulation (Fig. 1), it is possible that VprBP levels are modulated to titrate *Rag* transcript levels during G1 as well. Coordination of these mechanisms may enable fine control of V(D)J recombination activity within the G1 phase of the cell cycle, and would help explain how sequential V(D)J rearrangements, such as those occurring during receptor editing of the Ig light chain loci, are facilitated and regulated within G1 without requiring a cell cycle transition to suppress V(D)J recombination through the targeted degradation of RAG2.

The skewing of the B cell repertoire in VprBP$^{del/del}$Bcl2^{+} mice toward Igλ^{+} B cells, the association of this phenotype with increased κ-deletion and skewed Vκ rearrangement to Jκ5, and the subsequent finding that RAG1 protein levels are elevated in cultured B cells from these animals is reminiscent of findings from the Koralov group showing that loss of DGCR8 leads to transcriptional upregulation of *Rag* expression and increased receptor editing due to loss of miRNA-mediated suppression of PTEN (25). We were therefore interested in determining whether the phenotypes observed in VprBP$^{del/del}$Bcl2^{+} mice could be attributed to a secondary effect of the loss of Dicer. While loss of VprBP expression does lead to loss of Dicer (the implications of which are discussed further below), our direct comparison of VprBP$^{del/del}$Bcl2^{+} mice and Dicer$^{del/del}$Bcl2^{+} mice rules out this possibility by showing that loss of VprBP in VprBP$^{del/del}$Bcl2^{+} mice does not lead to transcriptional upregulation of *Rag* expression, and that loss of Dicer in Dicer$^{del/del}$Bcl2^{+} mice does not increase RAG1 protein levels in cultured BM cells from these animals. Our observation that RAG1 is present in VprBP$^{del/del}$Bcl2^{+} splenic B cells despite *Rag1* transcript levels being comparable to VprBP$^{fl/fl}$Bcl2^{+} cells (Fig. 2I) most likely reflects persistence of RAG1 from earlier developmental stages resulting from a complete loss of RAG1 turnover. Taken together, these data argue that VprBP and Dicer regulate RAG1 expression through distinct mechanisms: Dicer controls RAG1 expression indirectly at the transcriptional level via miRNA-mediated suppression of PTEN, and VprBP controls RAG1 expression at the post-transcriptional level by mediating its proteasome-dependent turnover. Furthermore, these distinct mechanisms may operate at different stages of B cell development, with regulation of PTEN expression by miRNAs being critical in transitional and mature B cells, but not in the bone marrow. This is consistent with the observation that cultured BM cells from Dicer$^{del/del}$Bcl2^{+} mice do not exhibit evidence of *Rag* transcriptional upregulation, as well as previous studies showing that deletion of PTEN does not rescue early B cell development in mice lacking miRNAs that target *Pten* mRNA (55).

This notion is further supported by our observation that, while marks of receptor editing are elevated in both VprBP$^{del/del}$Bcl2^{+} and Dicer$^{del/del}$Bcl2^{+} splenic B cells, this is only the case for bone marrow pre-B cells of the former knockout strain (Fig. 2E and 3F). Our experiments also revealed an overall reduction in Vκ-Jκ rearrangements in Dicer$^{del/del}$Bcl2^{+} pre-B cells, in the absence of a large effect on Vλ-Jλ rearrangement (Fig. 3F). A study from the Schlissel group (56) reported that expression of miR-290-5p and miR-292-5p is induced

at the pro- to pre-B cell transition, and that these miRNAs promote germline transcription of the *Igk* locus, which is strongly correlated with initiation of Igκ rearrangement (32). Thus, it is possible that loss of miR-290-5p and miR-292-5p results in impaired Vκ-Jκ rearrangement in Dicer$^{del/del}$Bcl2^{+} pre-B cells, and may even contribute to the skewing in the Igκ:Igλ ratio on the miRNA-deficient genetic background (Fig. 2; (25)). Further work will be required to investigate these possibilities.

Interestingly, despite the absence of Dicer and the elevation of PTEN in splenic B cells from VprBP$^{del/del}$Bcl2^{+} mice, we did not observe any increase in *Rag1* or *Rag2* transcript. This finding is also consistent with the absence of *Rag* transcriptional upregulation upon IL-7 withdrawal in BM cultures from VprBP$^{del/del}$Bcl2^{+} mice (Fig. 1E). These data together suggest that VprBP has a secondary role in regulating *Rag* transcription downstream of PTEN/PI3K. The mechanism underlying this observation remains to be determined.

Finally, the finding that loss of VprBP leads to a profound, transcription-independent loss of Dicer protein in B cell progenitors contrasts strikingly with reports that VprBP targets Dicer for degradation via the CRL4^{VprBP} complex in response to certain stimuli (36, 37). If this model were true in B cells, one might have expected that Dicer protein levels would *increase* upon loss of VprBP. The discrepancy between our findings and these previous reports may be attributed to the involvement of specific stimuli to induce Dicer degradation that are not recapitulated in the cultured BM cells used in this work. Specifically, in the study by Klockow *et al.* (36), Dicer degradation was shown to be caused by hijacking of the CRL4^{VprBP} complex by the HIV-1 accessory factor Vpr. Whether all Vpr-directed substrates are also physiological substrates of CRL4^{VprBP} remains unclear, and thus it is possible that VprBP only mediates Dicer degradation in the context of HIV infection (57, 58). In the study by Ren *et al.* (37), Dicer degradation was elicited by stimulation of HCT116 colon cancer cells with toll-like receptor ligands and IL-6. Thus, it is possible that VprBP functions to maintain Dicer levels via a mechanism that is restricted to B cells or lymphocytes. Further studies will be needed to investigate these possibilities. In any case, given the pleotropic roles attributed to VprBP (reviewed in (43)) and the findings reported here and elsewhere (36, 37) that the Dicer levels may be regulated by VprBP, some caution is warranted in interpreting results of experiments in which VprBP levels are suppressed using knock-down or knock-out approaches due to potential secondary effects caused by changes in cellular Dicer levels.

Acknowledgments

The authors also thank Dr. Sleckman for providing A70 cells, and Dr. Schatz and Elizabeth Corbett for providing anti-RAG1 antibody.

This work was supported by a grant to P.C.S. from the National Institutes of Health (NIH) (R01GM102487) and by revenue from Nebraska's excise tax on cigarettes awarded to Creighton University through the Nebraska Department of Health & Human Services (DHHS). NIH funding to support research laboratory construction (C06 RR17417-01), the Creighton University Animal Resource Facility (G20RR024001), the acquisition of the GE Healthcare Typhoon 9410 Variable Mode Imager (S10RR027352) and the Bio-Rad ZE5 Cell Analyzer (3R01GM102487-03S1) are gratefully acknowledged. This publication's contents represent the view(s) of the author(s) and do not necessarily represent the official views of the State of Nebraska, DHHS, or the NIH.

Abbreviations

VprBP	Viral protein r Binding Protein
Cul4	Cullin 4
DDB1	DNA damage-binding protein 1
DCAF1	DDB1- and CUL4-associated factor 1
RING	Really Interesting New Gene
CRL4	Cul4-RING E3 ubiquitin ligase
NTR	amino-terminal region
RSS	recombination signal sequence
PTEN	phosphatase and tensin homolog
DGCR8	DiGeorge critical region 8
PI3K	phosphoinositide-3-kinase
BM	bone marrow
BAFF	B cell activating factor
NAE	NEDD8 activating E1 enzyme
IRS	intron recombining sequence
RS	recombining sequence
CHX	cycloheximide

References

1. Schatz DG, Swanson PC. V(D)J Recombination: Mechanisms of Initiation. Annual Review Genetics. 2011; 45:167–202.
2. Schatz DG, Oettinger MA, Baltimore D. The V(D)J recombination activating gene, RAG-1. Cell. 1989; 59:1035–1048. [PubMed: 2598259]
3. Oettinger MA, Schatz DG, Gorka C, Baltimore D. RAG-1 and RAG-2, adjacent genes that synergistically activate V(D)J recombination. Science. 1990; 248:1517–1523. [PubMed: 2360047]
4. Silver DP, Spanopoulou E, Mulligan RC, Baltimore D. Dispensable sequence motifs in the RAG-1 and RAG-2 genes for plasmid V(D)J recombination. Proc Natl Acad Sci U S A. 1993; 90:6100–6104. [PubMed: 8327489]
5. Kirch SA, Sudarsanam P, Oettinger MA. Regions of RAG1 protein critical for V(D)J recombination. Eur J Immunol. 1996; 26:886–891. [PubMed: 8625984]
6. Roman CA, Cherry SR, Baltimore D. Complementation of V(D)J recombination deficiency in RAG-1(−/−) B cells reveals a requirement for novel elements in the N-terminus of RAG-1. Immunity. 1997; 7:13–24. [PubMed: 9252116]
7. Sekiguchi JA, Whitlow S, Alt FW. Increased accumulation of hybrid V(D)J joins in cells expressing truncated versus full-length RAGs. Mol Cell. 2001; 8:1383–1390. [PubMed: 11779512]

8. Dudley DD, Sekiguchi J, Zhu C, Sadofsky MJ, Whitlow S, DeVido J, Monroe RJ, Bassing CH, Alt FW. Impaired V(D)J recombination and lymphocyte development in core RAG1-expressing mice. J Exp Med. 2003; 198:1439–1450. [PubMed: 14581608]
9. Talukder SR, Dudley DD, Alt FW, Takahama Y, Akamatsu Y. Increased frequency of aberrant V(D)J recombination products in core RAG-expressing mice. Nucleic Acids Res. 2004; 32:4539–4549. [PubMed: 15328366]
10. Yurchenko V, Xue Z, Sadofsky M. The RAG1 N-terminal domain is an E3 ubiquitin ligase. Genes Dev. 2003; 17:581–585. [PubMed: 12629039]
11. Deshaies RJ, Joazeiro CA. RING domain E3 ubiquitin ligases. Annu Rev Biochem. 2009; 78:399–434. [PubMed: 19489725]
12. Jones JM, Gellert M. Autoubiquitylation of the V(D)J recombinase protein RAG1. Proc Natl Acad Sci U S A. 2003; 100:15446–15451. [PubMed: 14671314]
13. Simkus C, Bhattacharyya A, Zhou M, Veenstra TD, Jones JM. Correlation between recombinase activating gene 1 ubiquitin ligase activity and V(D)J recombination. Immunology. 2009; 128:206–217. [PubMed: 19740377]
14. Singh SK, Gellert M. Role of RAG1 autoubiquitination in V(D)J recombination. Proc Natl Acad Sci U S A. 2015; 112:8579–8583. [PubMed: 26124138]
15. Simkus C, Makiya M, Jones JM. Karyopherin alpha 1 is a putative substrate of the RAG1 ubiquitin ligase. Mol Immunol. 2009; 46:1319–1325. [PubMed: 19118899]
16. Grazini U, Zanardi F, Citterio E, Casola S, Goding CR, McBlane F. The RING domain of RAG1 ubiquitylates histone H3: a novel activity in chromatin-mediated regulation of V(D)J joining. Mol Cell. 2010; 37:282–293. [PubMed: 20122409]
17. Jones JM, Bhattacharyya A, Simkus C, Vallieres B, Veenstra TD, Zhou M. The RAG1 V(D)J recombinase/ubiquitin ligase promotes ubiquitylation of acetylated, phosphorylated histone 3.3. Immunology Letters. 2011; 136:156–162. [PubMed: 21256161]
18. Coster G, Gold A, Chen D, Schatz DG, Goldberg M. A Dual Interaction between the DNA Damage Response Protein MDC1 and the RAG1 Subunit of the V(D)J Recombinase. Journal of Biological Chemistry. 2012; 287:36488–36498. [PubMed: 22942284]
19. Maitra R, Sadofsky MJ. A WW-like module in the RAG1 N-terminal domain contributes to previously unidentified protein-protein interactions. Nucleic Acids Res. 2009; 37:3301–3309. [PubMed: 19324890]
20. Raval P, Kriatchko AN, Kumar S, Swanson PC. Evidence for Ku70/Ku80 association with full-length RAG1. Nucleic Acids Res. 2008; 36:2060–2072. [PubMed: 18281312]
21. Kassmeier MD, Mondal K, Palmer VL, Raval P, Kumar S, Perry GA, Anderson DK, Ciborowski P, Jackson S, Xiong Y, Swanson PC. VprBP binds full-length RAG1 and is required for B-cell development and V(D)J recombination fidelity. EMBO J. 2012; 31:945–958. [PubMed: 22157821]
22. Hobeika E, Thiemann S, Storch B, Jumaa H, Nielsen PJ, Pelanda R, Reth M. Testing gene function early in the B cell lineage in mb1-cre mice. Proc Natl Acad Sci U S A. 2006; 103:13789–13794. [PubMed: 16940357]
23. Palmer VL, Aziz-Seible R, Kassmeier MD, Rothermund M, Perry GA, Swanson PC. VprBP Is Required for Efficient Editing and Selection of Igκ+ B Cells, but Is Dispensable for Igλ+ and Marginal Zone B Cell Maturation and Selection. Journal of Immunology. 2015; 195:1524–1537.
24. Nemazee D. Mechanisms of central tolerance for B cells. Nature Reviews Immunology. 2017; 17:281–294.
25. Coffre M, Benhamou D, Riess D, Blumenberg L, Snetkova V, Hines MJ, Chakraborty T, Bajwa S, Jensen K, Chong MMW, Getu L, Silverman GJ, Blelloch R, Littman DR, Calado D, Melamed D, Skok JA, Rajewsky K, Koralov SB. miRNAs Are Essential for the Regulation of the PI3K/AKT/FOXO Pathway and Receptor Editing during B Cell Maturation. Cell Reports. 2016; 17:2271–2285. [PubMed: 27880903]
26. Winter J, Jung S, Keller S, Gregory RI, Diederichs S. Many roads to maturity: microRNA biogenesis pathways and their regulation. Nature Cell Biology. 2009; 11:228–234. [PubMed: 19255566]
27. McCall CM, Miliani de Marval PL, Chastain PD 2nd, Jackson SC, He YJ, Kotake Y, Cook JG, Xiong Y. Human immunodeficiency virus type 1 Vpr-binding protein VprBP, a WD40 protein

associated with the DDB1-CUL4 E3 ubiquitin ligase, is essential for DNA replication and embryonic development. Mol Cell Biol. 2008; 28:5621–5633. [PubMed: 18606781]

28. Harfe BD, McManus MT, Mansfield JH, Hornstein E, Tabin CJ. The RNaseIII enzyme Dicer is required for morphogenesis but not patterning of the vertebrate limb. Proc Natl Acad Sci U S A. 2005; 102:10898–10903. [PubMed: 16040801]
29. Holl TM, Haynes BF, Kelsoe G. Stromal cell independent B cell development in vitro: Generation and recovery of autoreactive clones. Journal of Immunological Methods. 2010; 354:53–67. [PubMed: 20109461]
30. Hassaballa AE V, Palmer L, Anderson DK, Kassmeier MD, Nganga VK, Parks KW, Volkmer DL, Perry GA, Swanson PC. Accumulation of B1-like B cells in transgenic mice over-expressing catalytically inactive RAG1 in the periphery. Immunology. 2011; 134:469–486. [PubMed: 22044391]
31. Amin RH, Schlissel MS. Foxo1 directly regulates the transcription of recombination-activating genes during B cell development. Nat Immunol. 2008; 9:613–622. [PubMed: 18469817]
32. Schlissel MS, Baltimore D. Activation of Immunoglobulin Kappa Gene Rearrangement Correlates with Induction of Germline Kappa Gene-Transcription. Cell. 1989; 58:1001–1007. [PubMed: 2505932]
33. Bredemeyer AL, Sharma GG, Huang CY, Helmink BA, Walker LM, Khor KC, Nuskey B, Sullivan KE, Pandita TK, Bassing CH, Sleckman BP. ATM stabilizes DNA double-strand-break complexes during V(D)J recombination. Nature. 2006; 442:466–470. [PubMed: 16799570]
34. Ochiai K, Maienschein-Cline M, Mandal M, Triggs JR, Bertolino E, Sciammas R, Dinner AR, Clark MR, Singh H. A self-reinforcing regulatory network triggered by limiting IL-7 activates pre-BCR signaling and differentiation. Nat Immunol. 2012; 13:300–307. [PubMed: 22267219]
35. Johnson K, Hashimshony T, Sawai CM, Pongubala JMR, Skok JA, Aifantis L, Singh H. Regulation of immunoglobulin light-chain recombination by the transcription factor IRF-4 and the attenuation of interleukin-7 signaling. Immunity. 2008; 28:335–345. [PubMed: 18280186]
36. Klockow LC, Sharifi HJ, Wen XY, Flagg M, Furuya AKM, Nekorchuk M, de Noronha CMC. The HIV-1 protein Vpr targets the endoribonuclease Dicer for proteasomal degradation to boost macrophage infection. Virology. 2013; 444:191–202. [PubMed: 23849790]
37. Ren WG, Shen SR, Sun ZQ, Shu P, Shen XH, Bu CB, Ai FY, Zhang XM, Tang AL, Tian L, Li GY, Li XY, Ma J. Jak-STAT3 pathway triggers DICER1 for proteasomal degradation by ubiquitin ligase complex of CUL4A(DCAF1) to promote colon cancer development. Cancer Letters. 2016; 375:209–220. [PubMed: 26965998]
38. Koralov SB, Muljo SA, Galler GR, Krek A, Chakraborty T, Kanellopoulou C, Jensen K, Cobb BS, Merkenschlager M, Rajewsky N, Rajewsky K. Dicer ablation affects antibody diversity and cell survival in the B lymphocyte lineage. Cell. 2008; 132:860–874. [PubMed: 18329371]
39. Shimizu T, Iwasato T, Yamagishi H. Deletions of Immunoglobulin C-Kappa Region Characterized by the Circular Excision Products in Mouse Splenocytes. Journal of Experimental Medicine. 1991; 173:1065–1072. [PubMed: 1902500]
40. Grawunder U, Schatz DG, Leu TMJ, Rolink A, Melchers F. The half-life of RAG-1 protein in precursor B cells is increased in the absence of RAG-2 expression. Journal of Experimental Medicine. 1996; 183:1731–1737. [PubMed: 8666930]
41. Ochodnicka-Mackovicova K, Bahjat M, Maas C, van der Veen A, Bloedjes TA, de Bruin AM, van Andel H, Schrader CE, Hendriks RW, Verhoeyen E, Bende RJ, van Noesel CJM, Guikema JEJ. The DNA Damage Response Regulates RAG1/2 Expression in Pre-B Cells through ATM-FOXO1 Signaling. Journal of Immunology. 2016; 197:2918–2929.
42. Sadofsky MJ, Hesse JE, McBlane JF, Gellert M. Expression and V(D)J recombination activity of mutated RAG-1 proteins. Nucleic Acids Res. 1993; 21:5644–5650. [PubMed: 8284210]
43. Nakagawa T, Mondal K, Swanson PC. VprBP (DCAF1): a promiscuous substrate recognition subunit that incorporates into both RING-family CRL4 and HECT-family EDD/UBR5 E3 ubiquitin ligases. BMC Mol Biol. 2013; 14:22. [PubMed: 24028781]
44. Soucy TA, Smith PG, Milhollen MA, Berger AJ, Gavin JM, Adhikari S, Brownell JE, Burke KE, Cardin DP, Critchley S, Cullis CA, Doucette A, Garnsey JJ, Gaulin JL, Gershman RE, Lublinsky AR, McDonald A, Mizutani H, Narayanan U, Olhava EJ, Peluso S, Rezaei M, Sintchak MD,

Talreja T, Thomas MP, Traore T, Vyskocil S, Weatherhead GS, Yu J, Zhang J, Dick LR, Claiborne CF, Rolfe M, Bolen JB, Langston SP. An inhibitor of NEDD8-activating enzyme as a new approach to treat cancer. Nature. 2009; 458:732–U767. [PubMed: 19360080]

45. Duda DM, Borg LA, Scott DC, Hunt HW, Hammel M, Schulman BA. Structural insights into NEDD8 activation of Cullin-RING ligases: Conformational control of conjugation. Cell. 2008; 134:995–1006. [PubMed: 18805092]
46. Jones J, Wu K, Yang YY, Guerrero C, Nillegoda N, Pan ZQ, Huang L. A targeted proteomic analysis of the ubiquitin-like modifier Nedd8 and associated proteins. Journal of Proteome Research. 2008; 7:1274–1287. [PubMed: 18247557]
47. Pan ZQ, Kentsis A, Dias DC, Yamoah K, Wu K. Nedd8 on cullin: building an expressway to protein destruction. Oncogene. 2004; 23:1985–1997. [PubMed: 15021886]
48. Adams J V, Palombella J, Sausville EA, Johnson J, Destree A, Lazarus DD, Maas J, Pien CS, Prakash S, Elliott PJ. Proteasome inhibitors: A novel class of potent and effective antitumor agents. Cancer Research. 1999; 59:2615–2622. [PubMed: 10363983]
49. Muljo SA, Schlissel MS. A small molecule Abl kinase inhibitor induces differentiation of Abelson virus-transformed pre-B cell lines. Nat Immunol. 2003; 4:31–37. [PubMed: 12469118]
50. Zhang YH, Shetty K, Surleac MD, Petrescu AJ, Schatz DG. Mapping and Quantitation of the Interaction between the Recombination Activating Gene Proteins RAG1 and RAG2. Journal of Biological Chemistry. 2015; 290:11802–11817. [PubMed: 25745109]
51. Verkoczy L, Ait-Azzouzene D, Skog P, Martensson A, Lang J, Duong B, Nemazee D. A role for nuclear factor kappa B/rel transcription factors in the regulation of the recombinase activator genes. Immunity. 2005; 22:519–531. [PubMed: 15845455]
52. Li Z, Dordai DI, Lee J, Desiderio S. A conserved degradation signal regulates RAG-2 accumulation during cell division and links V(D)J recombination to the cell cycle. Immunity. 1996; 5:575–589. [PubMed: 8986717]
53. Jiang H, Chang FC, Ross AE, Lee J, Nakayama K, Desiderio S. Ubiquitylation of RAG-2 by Skp2-SCF links destruction of the V(D)J recombinase to the cell cycle. Mol Cell. 2005; 18:699–709. [PubMed: 15949444]
54. Fisher MR, Rivera-Reyes A, Bloch NB, Schatz DG, Bassing CH. Immature Lymphocytes Inhibit Rag1 and Rag2 Transcription and V(D)J Recombination in Response to DNA Double-Strand Breaks. Journal of Immunology. 2017; 198:2943–2956.
55. Lai MY, Gonzalez-Martin A, Cooper AB, Oda H, Jin HY, Shepherd J, He LL, Zhu J, Nemazee D, Xiao CC. Regulation of B-cell development and tolerance by different members of the miR-17 similar to 92 family microRNAs. Nature Communications. 2016; 7:12207.
56. Garcia PB, Cai A, Bates JG, Nolla H, Schlissel MS. miR290-5p/292-5p Activate the Immunoglobulin kappa Locus in B Cell Development. Plos One. 2012; 7:e43805. [PubMed: 22928038]
57. Hrecka K, Gierszewska M, Srivastava S, Kozaczkiewicz L, Swanson SK, Florens L, Washburn MP, Skowronski J. Lentiviral Vpr usurps Cul4-DDB1[VprBP] E3 ubiquitin ligase to modulate cell cycle. Proc Natl Acad Sci U S A. 2007; 104:11778–11783. [PubMed: 17609381]
58. Wen X, Duus KM, Friedrich TD, de Noronha CM. The HIV1 protein Vpr acts to promote G2 cell cycle arrest by engaging a DDB1 and Cullin4A-containing ubiquitin ligase complex using VprBP/DCAF1 as an adaptor. J Biol Chem. 2007; 282:27046–27057. [PubMed: 17620334]

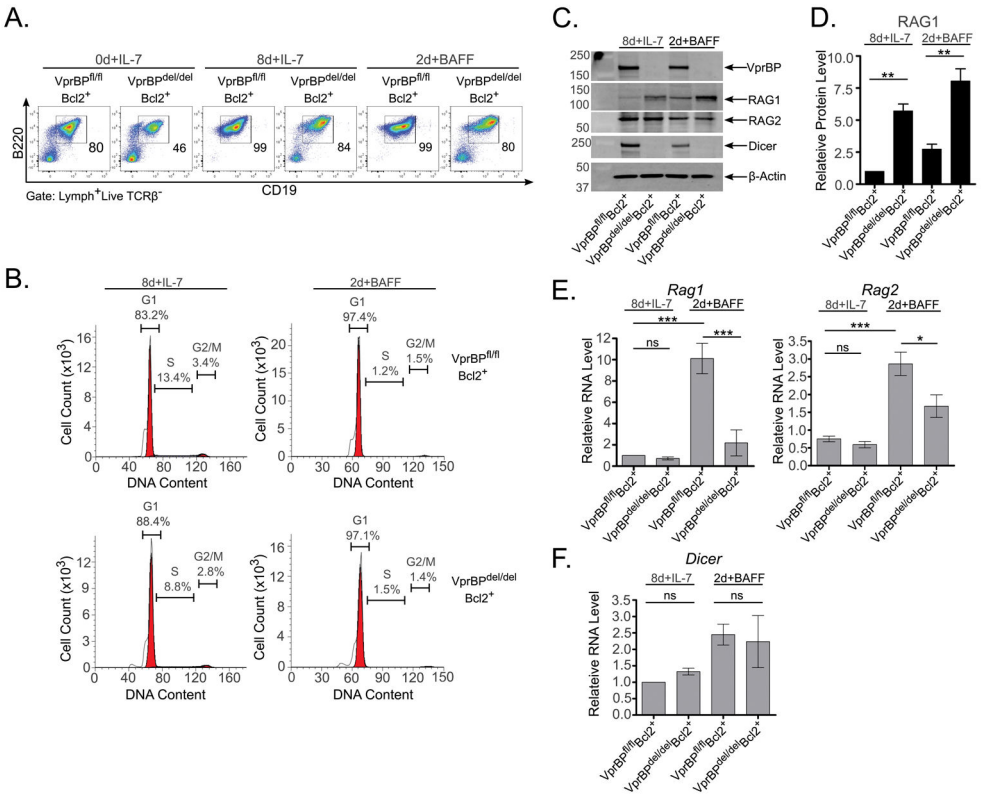

Figure 1. VprBP controls expression of Dicer and RAG1 in developing B cells

(A) BM cells from VprBP$^{fl/fl}$Bcl2^{+} and VprBP$^{del/del}$Bcl2^{+} mice were cultured for 0d or 8d in the presence of IL-7 (0d or 8d+IL7) with or without subsequent IL-7 withdrawal and BAFF supplementation for 2d (2d+BAFF). Cells were analyzed by flow cytometry to detect surface expression of B220 and CD19. The percentages of gated B220^{+}CD19^{+} cells are representative of multiple experiments. (B) B cells enriched by magnetic sorting were stained with Vindelov's reagent for determination of cell cycle status. Percentage of cells in each cell cycle phase is shown. (C) Lysates prepared from cultured BM cells were subjected to SDS-PAGE and western blotting to detect the indicated proteins. (D) Western blot signal for RAG1 was quantified and normalized to the β-actin signal, with signal from the VprBP$^{fl/fl}$Bcl2^{+} 8d+IL-7 sample arbitrarily set to 1.0. Data are representative of two independent experiments. (E–F) RNA isolated from cultured BM cells was subjected to RT-qPCR to analyze transcript levels of *Rag1* and *Rag2* (E) or *Dicer* (F), using *Hprt* levels for normalization. Error bars represent the mean +/− SEM from three independent experiments. ***P<0.001 by one-way ANOVA with Bonferroni post-hoc correction. ns = not significant.

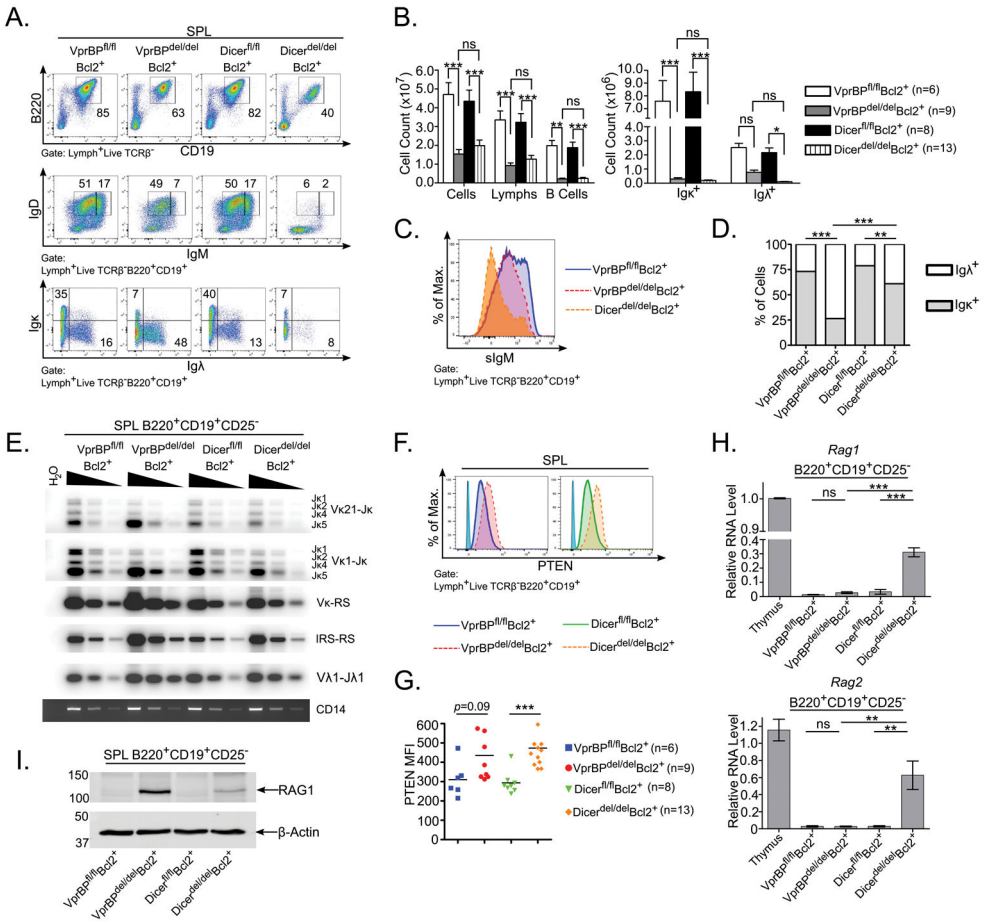

Figure 2. VprBP and Dicer restrain *Rag1* expression and receptor editing through distinct mechanisms

(A) Total splenocytes prepared from mice of the indicated genotypes were analyzed by flow cytometry for surface expression of CD19, B220, IgM, IgD, Igκ, and Igλ. (B) Total numbers of splenocytes, splenic lymphocytes**,** and splenic B cells (left panel), and total numbers of splenic Igκ$^+$ and Igλ$^+$ B cells (right panel) were determined for each genotype (n=6–13; listed at right), and displayed in bar graph format. Error bars represent the mean +/− SEM. *P<0.05, **P<0.01, ***P<0.001 by two-way ANOVA with Bonferroni post-hoc correction. (C) Representative plot comparing surface IgM (sIgM) staining for splenic B cells from mice of the indicated genotypes. (D) The proportion of Igκ$^+$ and Igλ$^+$ cells among total light-chain bearing splenic B cells was determined for the mice analyzed in panel B and is presented in bar graph format. (E) Splenic B220$^+$CD19$^+$CD25$^-$ B cells sorted from mice of the indicated genotypes were subjected to PCR and Southern blotting to amplify and detect specific V(D)J rearrangements listed to the right of each panel from 10000, 2500, or 625 cell equivalents of genomic DNA. Amplification of the non-rearranging CD14 locus serves as a loading control. (F) Splenocytes from mice of the indicated genotypes were analyzed by intracellular flow cytometry to detect PTEN expression. Staining with an isotype control antibody is shown (light blue peak). (G) Quantitation of the mean fluorescence intensity (MFI) was determined for each genotype (right panel; n=6–13). ***P<0.001 by one-way ANOVA with Bonferroni post-hoc correction. (H) Total RNA from splenic B cells sorted as

in panel A was subjected to RT-qPCR to detect *Rag1* and *Rag2* transcript. The level of *Rag1* and *Rag2* in VprBP$^{fl/fl}$Bcl2^{+} thymocytes was arbitrarily set to 1.0 for comparison. (I) Lysates prepared from sorted splenic B220^{+}CD19^{+}CD25^{-} B cells were probed by western blotting as in Fig. 1C.

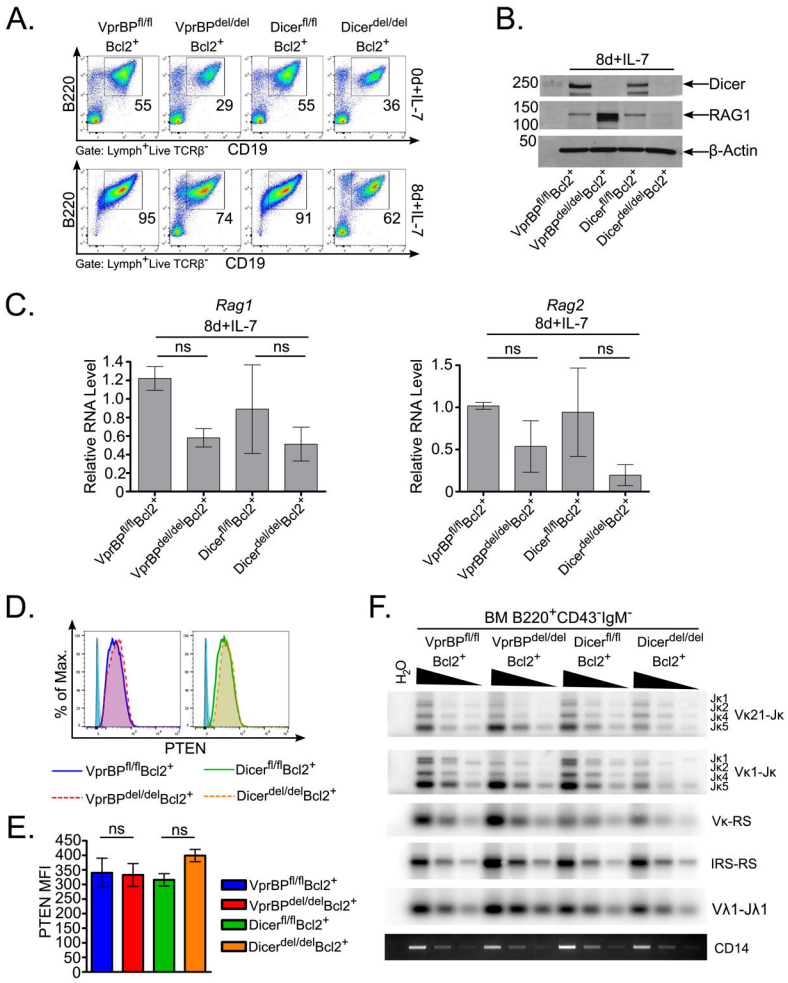

Figure 3. Loss of Dicer alone is insufficient to elevate RAG1 expression in cultured BM cells

(A) BM cells from mice of the indicated genotypes were cultured in the presence of IL-7 and analyzed as in Fig. 1A. Data are representative of three independent experiments. (B) Lysates prepared from 8d+IL-7 BM cultures were probed by Western blotting as in Fig. 1B. Data are representative of two independent experiments. (C) *Rag1* and *Rag2* transcript levels were compared between cultured BM cells from the indicated mice as in Fig. 1E. (D–E) Intracellular PTEN was detected by flow cytometry, and the mean fluorescence intensity (MFI) for PTEN staining was quantified as in Fig. 2F–G. (F) V(D)J rearrangements in sorted bone marrow pre-B cells ($B220^{+}CD43^{-}IgM^{-}$) were analyzed by PCR and southern blotting as in Fig. 2E. Error bars represent the mean +/− SEM for three independent experiments. ns = not significant by one-way ANOVA with Bonferroni post-hoc correction.

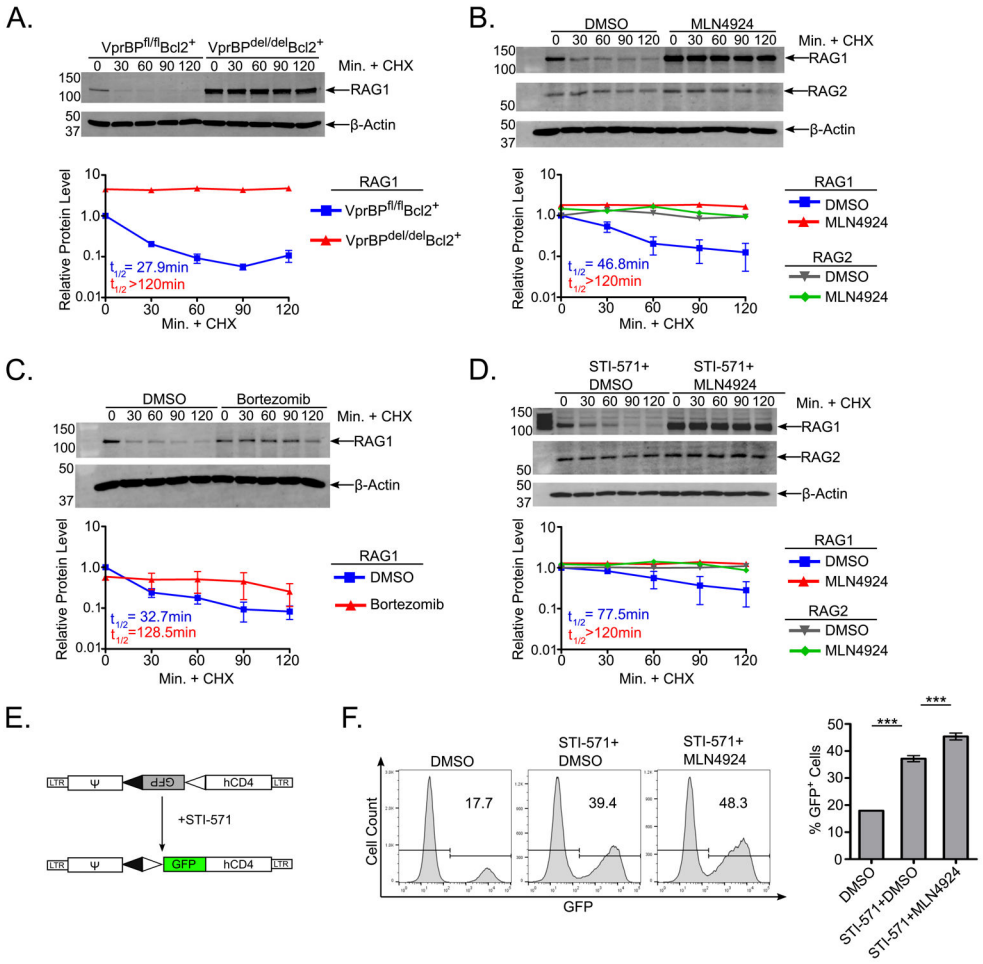

Figure 4. Loss of VprBP, or inhibition of the proteasome or NAE activity extends RAG1 half-life, and promotes increased V(D)J recombination

(A) (Top panel) BM cells from VprBP$^{fl/fl}$Bcl2^{+} or VprBP$^{del/del}$Bcl2^{+} mice were cultured for 8d in the presence of IL-7 and then subjected to IL-7 withdrawal and BAFF supplementation for 2d. For the final 2h of the culture period, cycloheximide was added (CHX, 20μg/mL), and cells were harvested at 30min intervals. Cell lysates were analyzed by western blotting as in Fig. 1C. Western blot signal for RAG1 was quantified and normalized to the β-actin signal as in Fig. 1D, and relative RAG1 signal at each time point was normalized to the sample at time 0. (B,C) BM cells from VprBP$^{fl/fl}$Bcl2^{+} mice were cultured as in panel A, and treated during the final 24h (after IL-7 withdrawal) with vehicle (DMSO), MLN4924 (3μM, panel B) or Bortezomib (5μM, panel C), with CHX added during the final 2h of culture. RAG1 and RAG2 protein levels were analyzed by western blotting and quantified as in panel A. (D) A70 cells were incubated in the presence of STI-571 for 48h and treated during the final 24h with vehicle (DMSO) or MLN4924, with CHX added during the final 2h of culture as in panels B and C. RAG1 and RAG2 were detected and quantified by western blotting as in panels B and C. (A–D) Error bars represent mean +/− SEM for two independent experiments. (E) Diagram of the pMX-INV reporter substrate. (F) A70 cells were treated with vehicle and inhibitor combinations as in panels D and analyzed by flow cytometry to detect GFP expression. Representative histograms from each treatment are

shown along with quantification of the percentage of GFP^+ cells from 3 independent experiments. Error bars represent mean +/− SEM from three independent experiments. ***P<0.001 by one-way ANOVA with Bonferroni post-hoc correction. ns = not significant.